Inorg. Chem. **2004**, *43*, 993–999

Insertion Reactions of *trans*-Mo(dmpe)$_2$(H)(NO) with Imines

Fupei Liang, Helmut W. Schmalle, and Heinz Berke*

Anorganisch-Chemisches Institut der Universität Zürich, Winterthurerstrasse 190, CH-8057 Zürich, Switzerland

Received April 25, 2003

The insertion chemistry of the hydride complex *trans*-Mo(dmpe)$_2$(H)(NO) (**1**) (dmpe = bis(dimethylphosphino)-ethane) with imines has been investigated. It was found that disubstituted aromatic imines RCH═NR′ (R, R′ = Ar) insert into the Mo–H bond of **1**, while a series of various mono- and other disubstituted imines do not react. The insertion products *trans*-Mo(dmpe)$_2$(NO)[NR′(CH$_2$R)] (R = R′ = Ph (**2**); R = Cp$_2$Fe, R′ = Ph (**3**); R = Ph, R′ = Cp$_2$Fe (**4**); R = 1-naphthyl, R′ = Ph (**5**)) have been isolated and fully characterized by elemental analysis, IR and NMR spectroscopy, and mass spectrometry. The imine PhCH═NC$_{10}$H$_7$ (C$_{10}$H$_7$ = 1-naphthyl) reacted with **1** establishing an equilibrium to produce the nonisolable complex *trans*-Mo(dmpe)$_2$(NO)[NC$_{10}$H$_7$(CH$_2$Ph)] (**6**). The equilibrium constant for this reaction has been derived from VT-NMR measurements, and the ΔH and ΔS values of this reaction were calculated to be -48.8 ± 0.4 kJ·mol^{-1} and -33 ± 1 J·K^{-1}·mol^{-1} reflecting a mild exothermic process and its associative nature. Single-crystal X-ray diffraction analyses were carried out on **2**–**5**.

Introduction

Insertion reactions of imines into transition metal−hydrogen bonds has been proposed to be a key step in catalytic homogeneous hydrogenations of imines.[1] However, so far insertion of imines into L$_n$M−H bonds leading to the metal amido intermediates have been observed only in rare cases as isolated steps.[1b,2] In addition and in contrast to the fact that main-group hydrides have frequently been utilized in hydride reductions of the carbon−nitrogen double bond,[3] applications of transition metal hydrides for related reductions of imines are up to now limited.[4] One reason for this obvious lack of activity may be that in the majority of cases the transition metal hydrogen bond possess too low polarity and concomitant nucleophilicity to react with the relatively inert C═N double bond. Nevertheless, it would be of great general interest to develop transition metal hydride systems capable of such insertions, since in contrast to main group compounds transition metal species could be envisaged to provide access to hydride species from a metal fragment and H_2 and thus could also operate on catalytic grounds. Such catalytic hydrogenations are known, but as indicated above, they are rare and quite often they lack activity and/or stability of the catalytic species. This contrasts the situation of related reductions of carbonyl functionalities with transition metal hydrides.[5a−e]Another avenue described by Noyori that involves 2-propanol as the sacrificial hydrogen source can also be utilized.[5f] Therefore, it was expected that by separate

* To whom correspondence should be addressed. E-mail: hberke@aci.unizh.ch.

(1) (a) Willoughby, C. A.; Buchwald, S. L. *J. Am. Chem. Soc.* **1994**, *116*, 8952. (b) Obora, Y.; Ohta, T.; Stern, C. L.; Marks, T. J. *J. Am. Chem. Soc.* **1997**, *119*, 3745. (c) James, B. R. *Catal. Today* **1997**, *37*, 209. (d) Kobayashi, S.; Ishitani, H. *Chem. Rev.* **1999**, *99*, 1069. (e) Blaser, H.-U.; Spindler, F. In *Comprehensive Asymmetric Catalysis*; Jacobsen, E. N., Plaltz, A., Yamamoto, H., Eds.; Springer-Verlag: New York, 1999; Vol. 1, p 247. (f) Magee, M. P.; Norton, J. R. *J. Am. Chem. Soc.* **2001**, *123*, 1778. (g) Herrera, V.; Muñoz, B.; Landaeta, V.; Canudas, N. *J. Mol. Catal., A* **2001**, *174*, 141. (h) Xiao, D.; Zhang, X. *Angew. Chem., Int. Ed.* **2001**, 3425. (i) Samec, J. S. M.; Bäckvall, J.-E. *Chem.—Eur. J.* **2002**, *8*, 2955.

(2) (a) Fryzuk, M. D.; Piers, W. E. *Organometallics* **1990**, *9*, 986. (b) Debad, J. D.; Legzdins, P.; Lumb, S. A.; Batchelor, R. J.; Einstein, W. B. *Organometallics* **1995**, *14*, 2543.

(3) (a) Oveman, L. E.; Freerks, R. L. *J. Org. Chem.* **1981**, *46*, 2833. (b) Jamada, K.; Takeda, M.; Iwakuma, T. *J. Chem. Soc., Perkin Trans.* **1983**, 265. (c) Polniaszek, R. P.; Kaufman, C. R. *J. Am. Chem. Soc.* **1989**, *111*, 4859. (d) Kavate, T.; Nakagawa, M.; Kakikawa T.; Hino, T. *Tetrahedron: Asymmetry* **1992**, 3, 227. (e) Sotomayor, N.; Dominguez, E.; Lete, E. *Synlett* **1993**, 431. (f) Tellitu, I.; Badia, D.; Dominguez, E.; Garcia, F. J. *Tetrahedron: Asymmetry* **1994**, *5*, 1567. (g) Kang, J.; Kim, J. B.; Cho, K. H.; Cho, B. T. *Tetrahedron: Asymmetry* **1997**, *8*, 657.

(4) Palagyi, J.; Nagy-Magos, Z.; Marko, L. *Transition Met. Chem.* **1985**, *10*, 336.

(5) (a) Darensbourg, M. Y.; Slater, S. G. *J. Am. Chem. Soc.* **1981**, *103*, 5914. (b) Slater, S. G.; Lusk, R.; Schumann, B. F.; Darensbourg, M. Y. *Organometallics* **1982**, *1*, 1662. (c) Gaus, P. L.; Kao, S. C.; Darensbourg, M. Y.; Arndt, L. W. *J. Am. Chem. Soc.* **1984**, *106*, 4752. (d) Gaus, P. L.; Kao, S. C.; Youngdahl, K.; Darensbourg, M. Y.; Arndt, L. W. *J. Am. Chem. Soc.* **1985**, 107, 2428. (e) Tooley, P. A.; Ovalles, C.; Kao, S. C.; Darensbourg, D. J.; Darensbourg, M. Y. *J. Am. Chem. Soc.* **1986**, *108*, 5465. (f) Noyori, R.; Hashiguchi, S. *Acc. Chem. Res.* **1997**, *30*, 97.

10.1021/ic030139l CCC: $27.50
Published on Web 01/09/2004

studies of stoichiometric imine insertions into transition metal−hydrogen bonds fundamental knowledge could be acquired of how to tune hydrides toward better catalytic performance among other possibilities via their coordination sphere.

In previous investigations we found that the insertion reaction of the hydride *mer*-Mo(CO)(H)(NO)(PMe_3)$_3$ related to **1** with *N*-benzylideneaniline is accessible; however, the reaction product could not be isolated and thus the structure of the product could not be definitely established.[6] We attributed the difficulty in the isolation of the product to an incomplete transformation caused by a too low activity of the hydride. Enforced reaction conditions led to decompositions. Prompted by this failure, we set out to study the synthesis and reactivity of hydrides with an enhanced polar character in the transition metal−hydrogen bond. In recent years our group has studied the chemistry of activated transition metal hydrides.[7] Systematic investigations allowed the conclusion that strong trans-influence ligands such as nitrosyl and carbyne groups tune the L_nM-H bond toward greater ionicity (hydridicity). A similar effect was seen upon increase of the number of strongly σ-donating cis phosphine substituents.[8] Following these lines we have recently prepared the complex *trans*-Mo(dmpe)$_2$(H)(NO) (dmpe = bis(dimethylphosphino)ethane),[9] a hydride complex with four cis phosphorus donors in the coordination sphere of the molybdenum center. It was found that this hydride indeed displayed the requested enhanced hydridic character.

Results and Discussions

Reaction of *trans*-Mo(dmpe)$_2$(H)(NO) (1) with Imines. Hydride **1** was synthesized by a procedure already reported by us.[9] Treatment of **1** with equimolar amounts of *N*-benzylideneaniline in toluene afforded the corresponding amido complex **2** (Scheme 1). The insertion reaction was found to proceed smoothly at room temperature and was complete after 24 h. The reaction conditions are much milder than those for the analogous reaction of *mer*-Mo(CO)(H)(NO)(PMe_3)$_3$,[6] presumably reflecting the increased hydridic character of **1**. However, the reaction took much longer time compared to the reaction of **1** with the C═O double bond of ketones,[9] for which the reactions lasted only 2−3 h indicating a general reluctance of imine double bonds to undergo insertion reactions. The insertion product **2** could easily be isolated as analytically pure yellow crystals in 81% yield after diffusion of pentane into a toluene solution of **2**.

Scheme 1

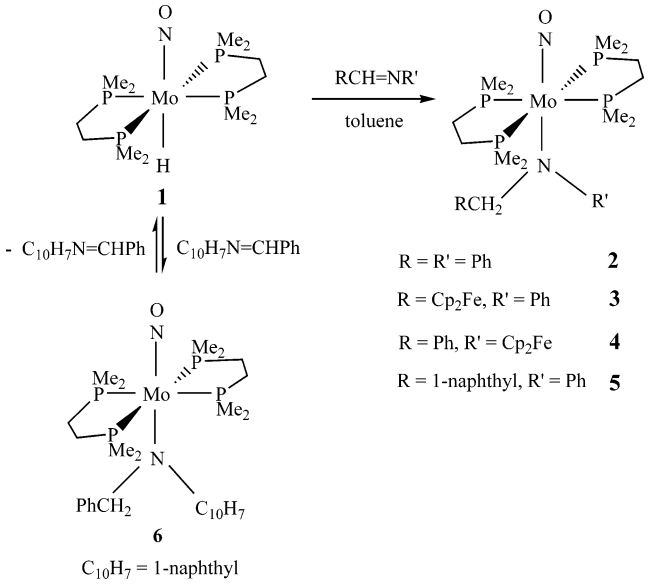

1 reacted also with *N*-ferrocenylideneaniline, *N*-benzylideneferrocenylamine, and *N*-1-naphthylideneaniline to produce the isolable amide complexes **3**−**5**, respectively (Scheme 1). However, all these reactions proceeded much slower than the reaction of *N*-benzylideneaniline. For example, reactions of **1** with *N*-ferrocenylideneaniline and *N*-1-naphthylideneaniline in toluene took about 5 days at room temperature. Heating facilitated the reactions, and at 65 °C they came to an end overnight. These reactivity differences were presumably due to enhanced steric influences of the substituents at the $C_{C=N}$ atom. The bulkier ferrocenyl and naphthyl groups in *N*-ferrocenylideneaniline and *N*-1-naphthylideneaniline hinder the hydride transfer step more. Reaction of **1** with *N*-benzylideneferrocenylamine took even 3 days to come to completion at 65 °C revealing that still more enforced conditions are required, in particular when compared to the reaction of its isomer, *N*-ferrocenylideneaniline. This difference in reactivity between these two compounds can presumably again be attributed to steric crowding at the nitrogen atom. In the transition state the ferrocenyl substituent at the forming amido faces decisive steric repulsion with the Mo(dmpe)$_2$(NO) fragment.

A related, but presumably more enhanced, steric hindrance now being related also to the product can be derived from the difference in reactivity of the two isomers *N*-1-naphthylideneaniline and *N*-benzylidene-1-naphthylamine. In contrast to the reaction with *N*-1-naphthylideneaniline, the reaction of **1** with *N*-benzylidene-1-naphthylamine turns out to be an equilibrium (Scheme 1) preventing the amido complex **6** from being isolated from the reaction mixture.

(6) Liang, F.; Jacobsen, H.; Schmalle, H. W.; Fox, T.; Berke, H. *Organometallics* **2000**, *19*, 1950.
(7) (a) van der Zeijden, A. A. H.; Veghini, D.; Berke, H. *Inorg. Chem.* **1992**, *31*, 5106. (b) van der Zeijden, A. A. H.; Berke, H. *Helv. Chim. Acta* **1992**, *75*, 513. (c) Nietlispach, D.; Bakhmutov, V. I.; Berke, H. *J. Am. Chem. Soc.* **1993**, *115*, 9191. (d) Bakhmutov, V. I.; Bürgi, T.; Burger, P.; Ruppli, U.; Berke, H. *Organometallics* **1994**, *13*, 4203. (e) Nietlispach, D.; Veghini, D.; Berke, H. *Helv. Chim. Acta* **1994**, *77*, 2197. (f) Shubina, E. S.; Belkova, N. V.; Krylov, A. N.; Vorontsov, E. V.; Epstein, L. M.; Gusev, D. G.; Niedermann, M.; Berke, H. *J. Am. Chem. Soc.* **1996**, *118*, 1105. (g) Belkova, N. V.; Shubina, E. S.; Ionidis, A. V.; Epstein, L. M.; Jacobsen, H.; Messmer, A.; Berke, H. *Inorg. Chem.* **1997**, *36*, 1522. (h) Gusev, D. G.; Llamazares, A.; Artus, G.; Jacobsen, H.; Berke, H. *Organometallics* **1999**, *18*, 75. (i) Messmer, A.; Jacobsen, H.; Berke, H. *Chem.—Eur. J.* **1999**, *5*, 3341. (j) Bannwart, E.; Jacobsen, H.; Furno, F.; Berke, H. *Organometallics* **2000**, *19*, 3605. (k) Furno, F.; Fox, T.; Schmalle, H. W.; Berke, H. *Organometallics* **2000**, *19*, 3620. (l) Höck, J.; Jacobsen, H.; Schmalle, H. W.; Artus, G. R. J.; Fox, T.; Amor, J. I.; Bäth, F.; Berke, H. *Organometallics* **2001**, *20*, 1533. (m) Furno, F.; Fox, T.; Alfonso, M.; Berke, H. *Eur. J. Inorg. Chem.* **2001**, 1559.
(8) (a) Berke, H.; Burger, P. *Comments Inorg. Chem.* **1994**, *16*, 279. (b) Jacobsen, H.; Berke, H. In *Recent Advences in Hydride Chemistry*; Poli, R., Peruzzini, M., Eds.; Elsevier: Amsterdam, 2001; p 89.
(9) Liang, F.; Schmalle, H. W.; Fox, T.; Berke, H. *Organometallics* **2003**, 22, 3382.

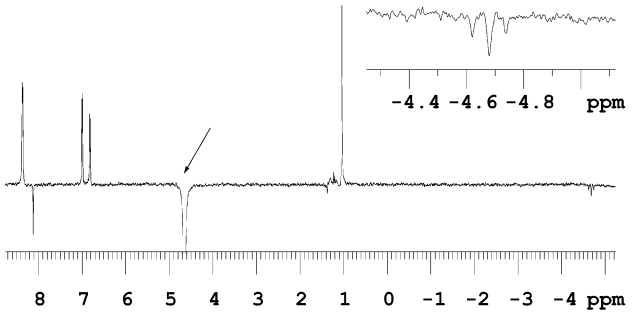

Figure 1. 1D-NOE ^{1}H NMR spectrum of the equilibrium reaction of **1** with (1-naphthyl)CH_2═NPh to yield **6** (Scheme 1) (C_7D_8, room temperature).

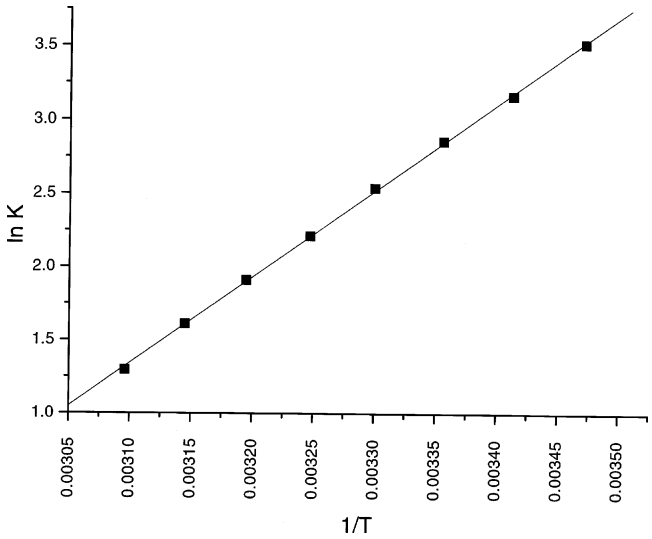

Figure 2. van't Hoff plot for the equilibrium reaction of **1** with (1-naphthyl)CH_2═NPh (Scheme 1). *K* values are from ^{31}P NMR in C_7D_8.

But the formation of **6** can clearly be deduced from the NMR spectra of the reaction mixture. In the ^{1}H NMR spectrum (C_7D_8) a singlet at 4.67 ppm can be attributed to the −NCH_2– protons. This assignment has been confirmed by an 1D-NOE experiment. When the signal at 4.67 ppm was irradiated, exchange with signals at 8.1 and −4.72 ppm (resonances for the −CH= group of the imine and the HMo atom, respectively) could be identified (Figure 1). The ^{31}P{^{1}H} spectrum displays besides the signal for **1** a singlet at 24.8 ppm, which belongs to **6**.

The temperature dependence of the equilibrium constant *K* of this reaction to **6** has been determined by NMR in C_7D_8. A van't Hoff plot is drawn out in Figure 2, which allowed for the calculation of DH and DS amounting to −48.8 ± 0.4 kJ·mol^{-1} and −33 ± 1 J·K^{-1}·mol^{-1}, respectively. The reaction is therefore only mildly exothermic, which is presumably similar but still a bit less on the exothermic side than the other cases of investigated inserting imines. Δ*H* for the reaction to **6** is smaller than that of **1** with Mo(dmpe)$_2$(NO)[(μ-OCH)$Re_2(CO)_9$],[9] where a Mo−O bond is newly installed. This can be attributed to a generally smaller Mo−N bond energy in comparison with the Mo−O bond.

The screening of the insertion capability of **1** with imines was extended to a series of other imines listed in Table 1. All these reactions were carried out as NMR experiments at room temperature or at 60−70 °C for 2 days in C7D_8 with a 10:1 stoichiometric ratio of the imine and **1**. However, no insertion reaction was observed for all these imines under the given conditions. The imines listed in Table 1 can be classified into three categories: C-disubstituted imines (entry a); *C*-phenyl- and *N*-alkyl-substituted imines (entry b); imines with a π-donor atom at the carbon terminus of the C═N moiety (entry c). These negative observations presumably allow us to generalize that hydride **1** preferably reacts with 1,2-diaryl-substituted imines.

Table 1. Imines Tested for Insertion with **1**

a	$_{Me2}$C═NCHMe$_2$; Me_2C═NPh; Ph(Me)C═NPh; Ph_2C═NPh; Ph_2C═NH
b	PhCH═NCH_2Ph; PhCH═NMe
c	2-methy-2-oxazoline; 1,5-diazabicyclo[2.2.2]octane; (Me_2N)$_2$C═NH

The possibility of an acceleration of such imine insertions of **1** in the presence of protic substrates, as it was found in many cases of insertion reactions of aldehydes or ketones with transition metal hydrides,[5,10] has been additionally probed. The relatively acidic OH species phenol, methyl alcohol, and ethyl alcohol were added to the reaction systems of **1** and the imines. However, insertions have not been detected; rather reactions of **1** with the acids occurred leading to evolution of dihydrogen and formation of the corresponding alkoxide complexes for both "reactive" and "nonreactive" imines of Table 1.

Characterization of Complexes 2−5. The insertion products **2**−**5** could be isolated as analytically pure compounds and have been fully characterized by elemental analysis, IR and NMR spectroscopy, and mass spectrometry. Selected spectroscopic features are discussed below.

Besides the signals for the phenyl ring protons of the amido moiety appearing in the range of 6.47−7.05 ppm and those for the methylene and methyl protons of the dmpe ligands between 1.05 and 1.35 ppm, the ^{1}H NMR spectrum of **2** shows a singlet at 4.28 ppm (C_6D_6) belonging to the newly formed N bound CH_2 group. In the ^{13}C{^{1}H} NMR the signal of this $C_{methylene}$ atom was found at 59.0 ppm as a quintet due to coupling with the four chemically equivalent dmpe phosphorus nuclei ($^3J_{CP}$ = 6 Hz). In contrast to the other sharp singlets for the C_{phenyl} atoms, a broadened signal was observed at 119.5 ppm for the phenyl C_{ipso} atom. The broadening is anticipated to be due to a small ^3J coupling with the phosphorus nuclei.

The ^{31}P{^{1}H} NMR spectra of the isomeric complexes **3** and **4** are very similar and comparable to **2** (24.8 ppm) indicated by singlets at 25.1 (**3)** and at 24.8 ppm (**4)**, while the ^{1}H and ^{13}C{^{1}H} NMR spectra show greater deviations reflecting the structural differences of both complexes. The ^{1}H NMR spectra of **3** and **4** in C_6D_6 display characteristic singlets at 4.06 and 3.34 ppm, respectively, which are assigned to their methylene protons. Their marked difference in chemical shift may be related to the difference in pyramidalization at the amido atom (vide infra). For **4** two signals belonging to the protons of the two Cp rings (the

(10) (a) Kundel, P.; Berke, H. *J. Organomet. Chem.* **1987**, *335*, 353. (b) van der Zeijden, A. A. H.; Bosch, H. W.; Berke, H. *Organometallics* **1992**, *11*, 2051. (c) Höck, J.; Fox. T.; Schmalle, H.; Berke, H. *Chimia* **1999**, *53*, 350. (d) Messmer, A. Ph.D. Thesis, University of Zurich, 1999.

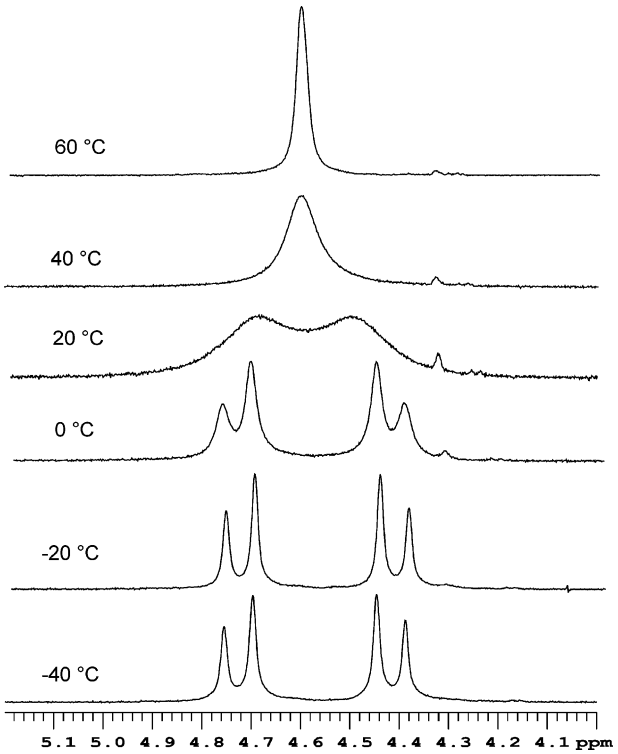

Figure 3. VT-^{1}H NMR spectra for the $-NCH_{2-}$ group of **5** in C_7D_8.

substituted Cp ring is denoted as Cp′) are found as a singlet at 3.88 ppm and a multiplet at 3.80 ppm with an intensity ratio of 5:4 (Cp and Cp′), whereas the related resonances for **3** appear as a singlet at 4.09 ppm and two triplets at 3.97 and 3.84 ppm, respectively. In the $^{13}C\{^1H\}$ NMR spectra of **3** and **4** the resonances for the $C_{methylene}$ atoms are found with a small chemical shift difference at 53.5 and 55.8, respectively. The ferrocenyl unit of **3** shows no P coupled signal exhibiting four singlets at 93.6 (Cp), 69.2, 68.8, and 65.8 ppm (all Cp′), while the resonances for the ferrocenyl rings of **4** show two singlets at 68.3 (Cp) and 60.9 ppm and a quintet at 62.3 ppm (both Cp′). The splitting of the latter signal confirms the vicinity of the Cp′ C_{ipso} atom of **4** to the metal phosphine moiety. Conversely and as expected from the substituent exchanged structure of both isomers, the C_{ipso} atom of the phenyl group of **3** shows P coupling (quintet at 120.6 ppm), while the signals for the other aromatic C nuclei appear as singlets, as do all C_{phenyl} resonances of **4**.

In the ^{1}H NMR spectrum of **5** (C_6D_6) the resonances of the $-NCH_{2-}$ protons were found as two broad singlets at 4.84 and 4.57 ppm, respectively, which is different from the corresponding resonances of **2**−**4** featuring just singlets. The appearance of two signals for **5** indicates hindered rotation of the naphthyl moiety rendering the two hydrogen atoms to be diasterotopic, and indeed their resonances display temperature-dependence (Figure 3). At low-temperature two doublets with a geminal coupling ($^2J_{HH}$ = 17 Hz at −40 °C) can be observed. At high temperature fast rotation of the naphthyl moiety on the NMR time scale occurs, which leads to equivalency of the two hydrogen atoms of the CH_2 group. In the $^{13}C\{^1H\}$ NMR spectrum of **5** (C_6D_6, room temperature) the resonance of the N bound methylene group appears at 56.2 ppm as a quintet with a C−P coupling constant of 7 Hz. The $^{31}P\{^1H\}$ NMR spectrum shows a singlet at 24.8 ppm. All these latter NMR data of **5** are comparable to those of the amido complexes **2**−**4**.

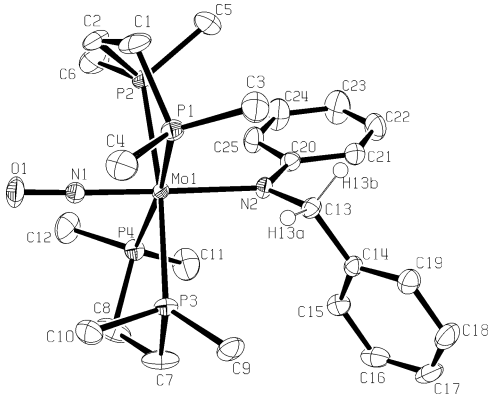

Figure 4. ORTEP plot of the structure of **2**. Displacement ellipsoids are drawn with 50% probability. All hydrogen atoms except for H13a and H13b are omitted for clarity.

Table 2. Selected Bond Lengths (Å) and Bond Angles (deg) of **2**

Mo(1)−N(1)	1.7916(15)	N(1)−Mo(1)−P(1)	86.32(5)
Mo(1)−N(2)	2.2421(14)	N(1)−Mo(1)−P(2)	84.97(5)
Mo(1)−P(1)	2.4982(5)	N(1)−Mo(1)−P(3)	87.87(5)
Mo(1)−P(2)	2.4781(6)	N(1)−Mo(1)−P(4)	85.62(5)
Mo(1)−P(3)	2.5020(6)	N(1)−Mo(1)−N(2)	177.46(6)
Mo(1)−P(4)	2.4946(5)	C(20)−N(2)−Mo(1)	130.00(12)
N(1)−O(1)	1.2255(19)	C(13)−N(2)−Mo(1)	115.72(11)
N(2)−C(20)	1.385(2)	C(20)−N(2)−C(13)	113.46(15)
N(2)−C(13)	1.463(2)	P(1)−Mo(1)−P(2)	77.997(19)
		P(3)−Mo(1)−P(4)	79.500(18)

Crystal Structures of Complexes 2−5. Crystals of **2** suitable for X-ray diffraction analysis were obtained by slow diffusion of pentane into a solution of the complex in toluene at room temperature. An ORTEP plot of **2** is given in Figure 4. The complex has a pseudooctahedral coordination geometry around the Mo center. The N_{NO}−Mo−P bond angles (Table 2) show that the phosphine ligands bend toward the nitrosyl group. This bending may be attributed to the steric repulsion[9] between the Mo(dmpe)$_2$(NO) fragment and the amido moiety. Presumably based on the same effect, an elongation of about 0.04 Å for the Mo−P bonds (Table 2, average 2.4932 Å) can be observed in comparison with the previously reported other complexes containing an Mo(dmpe)$_2$(NO) fragment.[9] The relatively long Mo(1)−N(2) (amido) bond length of 2.2421(14) Å in **2** can be primarily ascribed to the trans influence of the NO group. The N(2)−C(20) bond distance of 1.385(2) Å and the N(2)−C(13) distance of 1.463(2) Å are comparable to those found for N−C(sp^2) and N−C(sp^3) bonds in amido complexes.[11] The amido nitrogen exhibits a planar rather than a pyramidal geometry[12] with a sum of the three bond angles of around N(2) of 359.2°.

To further support and compare the structure of the isomericcomplexes **3** and **4** both complexes have been

(11) (a) Laplaza, C. E.; Odom, A. L.; Davis, W. M.; Cummins, C. C. *J. Am. Chem. Soc.* **1995**, *117*, 4999. (b) Laplaza, C. E.; Johnson, M. J. A.; Peters, J. C.; Odom, A. L, Kim, E.; Cummins, C. C.; George, G. N.; Pickering, I. J. *J. Am. Chem. Soc.* **1996**, *118*, 8623.
(12) (a) Chiu, K. W.; Wong, W.-K.; Wilkinson, G. *Polyhedron* **1982**, *1*, 37. (b) Dewey, M. A.; Arif, A. M.; Gladysz, J. A. *J. Chem. Soc., Chem. Commun.* **1991**, 712.

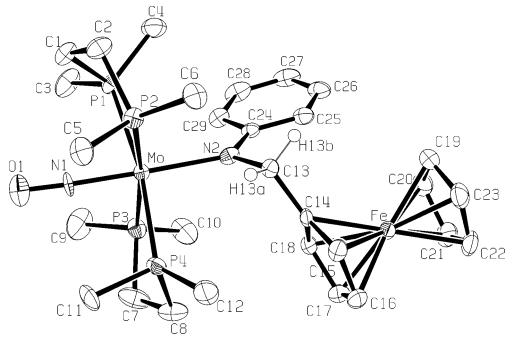

Figure 5. ORTEP plot of the structure of **3**. Displacement ellipsoids are drawn with 50% probability. The benzene solvate molecule and all hydrogen atoms except for H13a and H13b are omitted for clarity.

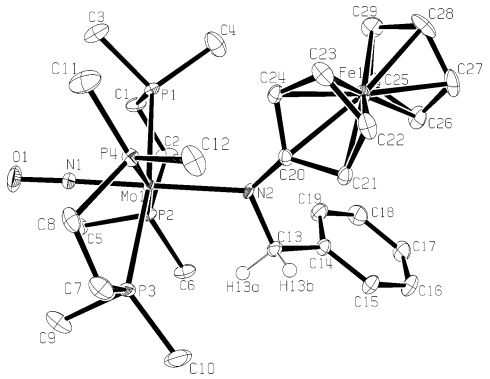

Figure 6. ORTEP plot of the structure of **4**. Displacement ellipsoids are drawn with 50% probability. All hydrogen atoms except for H13a and H13b are omitted for clarity.

Table 3. Selected Bond Lengths (Å) and Bond Angles (deg) of **3**[a]

Mo−N(1)	1.813(2)	N(1)−Mo−P(1)	82.91(8)
Mo−N(2)	2.253(2)	N(1)−Mo−P(2)	85.32(8)
Mo−P(1)	2.4916(7)	N(1)−Mo−P(3)	86.87(8)
Mo−P(2)	2.4733(7)	N(1)−Mo−P(4)	87.21(8)
Mo−P(3)	2.5056(7)	N(2)−Mo−P(1)	95.07(6)
Mo−P(4)	2.4965(7)	N(2)−Mo−P(2)	95.90(6)
N(1)−O(1)	1.193(3)	N(2)−Mo−P(3)	92.05(6)
N(2)−C(24)	1.388(3)	N(2)−Mo−P(4)	94.90(6)
N(2)−C(13)	1.472(3)	C(24)−N(2)−Mo	128.96(17)
Fe−C(14)	2.109(2)	C(13)−N(2)−Mo	117.28(15)
Fe−C(16)	2.031(3)	C(24)−N(2)−C(13)	113.3(2)
Fe−C(18)	2.071(3)	P(1)−Mo−P(2)	78.95(2)
Fe−C(21)	2.061(3)	P(3)−Mo−P(4)	79.15(3)
Fe−C(22)	2.047(3)	Cp(1)−Fe−Cp(2)	176.71(3)
Fe−Cp(1)	1.6649(4)		
Fe−Cp(2)	1.6591(4)		

[a] Cp(1) and Cp(2) refer to the centers of the gravity of the cyclopentadienyl rings C(14)−C(18) and C(19)−C(23), respectively.

subjected to crystallographic analyses. Diffusion of pentane into a benzene solution afforded suitable crystals of **3**, which crystallized as a benzene solvate. Suitable crystals of **4** were obtained by diffusion of pentane into a toluene solution. The ORTEP drawings of **3** and **4** are depicted in Figures 5 and 6, respectively. Selected bond lengths and angles are given in Table 3 for **3** and in Table 4 for **4**. Overall, the related bond distances and angles around the molybdenum centers of **3** and **4** are very close suggesting in particular similar binding strengths of the amido nitrogen atom to Mo in the two complexes. The only structural differences that can be detected, which are presumably too small and therefore not relevant in terms of thermodynamics, are the pyramidal angles at the nitrogen atoms of the amido units. **3** again

Table 4. Selected Bond Lengths (Å) and Bond Angles (deg) of **4**[a]

Mo(1)−N(1)	1.787(3)	N(1)−Mo(1)−P(1)	87.10(9)
Mo(1)−N(2)	2.240(2)	N(1)−Mo(1)−P(2)	86.67(9)
Mo(1)−P(1)	2.4987(8)	N(1)−Mo(1)−P(3)	83.85(9)
Mo(1)−P(2)	2.4900(8)	N(1)−Mo(1)−P(4)	84.53(9)
Mo(1)−P(3)	2.4999(9)	N(2)−Mo(1)−P(1)	93.34(7)
Mo(1)−P(4)	2.4756(8)	N(2)−Mo(1)−P(2)	94.66(7)
N(1)−O(1)	1.218(3)	N(2)−Mo(1)−P(3)	95.78(7)
N(2)−C(20)	1.367(4)	N(2)−Mo(1)−P(4)	94.14(7)
N(2)−C(13)	1.479(4)	C(20)−N(2)−Mo(1)	124.8(2)
Fe−C(20)	2.230(3)	C(13)−N(2)−Mo(1)	115.73(19)
Fe−C(22)	2.015(3)	C(20)−N(2)−C(13)	112.8(2)
Fe−C(24)	2.083(3)	P(1)−Mo(1)−P(2)	79.49(3)
Fe−C(27)	2.060(4)	P(3)−Mo(1)−P(4)	79.09(3)
Fe−C(29)	2.052(4)	Cp(1)−Fe−Cp(2)	177.06(3)
Fe−Cp(1)	1.6915(4)		
Fe−Cp(2)	1.6576(4)		

[a] Cp(1) and Cp(2) refer to the centers of the gravity of the cyclopentadienyl rings C(14)−C(18) and C(19)−C(23), respectively.

adopts a practically planar geometry at this atom with a sum of the three angles around N(2) of 359.5°. The amido nitrogen atom of **4** however shows a slight pyramidalization with a sum of the angles around N(2) of 353°. For the ferrocenyl fragment the Fe−C distances of **3** (2.031(3)−2.071(3) Å) are comparable to those of **4** (2.015(3)−2.083(3) Å) and to those found in ferrocene and its derivatives.[13] The Fe−C distances of the C_{ipso} atom of **4** (Fe−C(20), 2.230(3) Å) and the same one of **3** (Fe−C(14), 2.109(2) Å) are significantly elongated especially in **4**, which may be ascribed to steric repulsion with the substituents, i.e., the Mo(dmpe)$_2$(NO) fragment and the other residue of the amido group. Similar steric effects have previously been seen in complexes with congested substituents at the ferrocene ring.[14]

The bulky naphthyl moiety in **5** has been found to affect the ^{1}H NMR spectrum of newly formed $-NCH_2-$ group due to hindered rotation in solution. It was therefore of interest to see to what preferred conformation the spectral properties might be attributable to. **5** was subjected to an X-ray diffraction study. Suitable crystals were obtained by cooling a toluene solution to −30 °C for several weeks. Under the given conditions **5** crystallized as toluene solvate. The asymmetric unit of **5** contains two independent molecules, and in each molecule the Mo center is pseudooctahedrally coordinated similar to those of compounds **2**−**4**. The structural model of one of both independent molecules is shown in Figure 7. Selected bond distances and angles of both molecules are given in Table 5. A comparison of the bond distances and the bond angles around the Mo centers of **5** with those of **2**−**4** does not reveal significant deviations in the essential parts of the coordination geometries. Even the related bond lengths and angles around the practically planar amido nitrogen atom of **5** are almost the same as those of **2** and **3**. All these observations suggest that the bulkiness naphthyl moiety does not lead to significant changes of the structural parameters of **5** in the solid state. The conformations of the aromatic rings are very similar in both indepen-

(13) (a) Bracci, M.; Ercolani, C.; Floris, B.; Bassetti, M.; Chiesi-Villa, A.; Guastini, C. *J. Chem. Soc., Dalton Trans.* **1990**, 1357. (b) Silver, J.; Miller, J. R.; Houlton, A.; Ahmet, M. T. *J. Chem. Soc., Dalton, Trans.* **1994**, 3355. (c) Barranco, E. M.; Gimeno, M. C.; Jones, P. G.; Laguna, A.; Villacampa, M. D. *Inorg. Chem.* **1999**, *38*, 702.

(14) Roberts, R. M. G.; Silver, J.; Yamin, B. M.; Drew, M. G. B.; Eberhardt, U. *J. Chem. Soc., Dalton Trans.* **1988**, 1549.

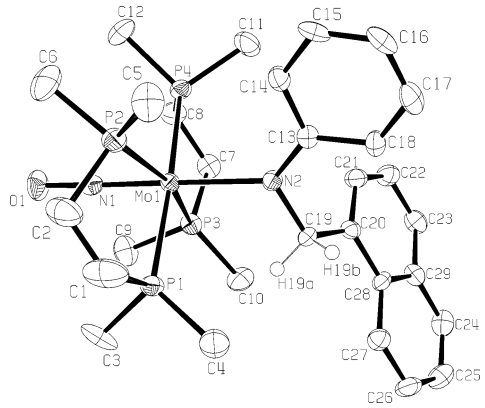

Figure 7. ORTEP plot of the structure of **5**. Displacement ellipsoids are drawn with 50% probability. The benzene solvate molecules and all hydrogen atoms except for H19a and H19b are omitted for clarity.

Table 5. Selected Bond Lengths (Å) and Bond Angles (deg) of **5**

Mo(1)−N(1)	1.778(4)	N(1)−Mo(1)−P(1)	87.92(13)
Mo(1)−N(2)	2.251(4)	N(1)−Mo(1)−P(2)	79.40(13)
Mo(1)−P(1)	2.4883(14)	N(1)−Mo(1)−P(3)	85.39(13)
Mo(1)−P(2)	2.5142(14)	N(1)−Mo(1)−P(4)	88.41(13)
Mo(1)−P(3)	2.4888(13)	N(1)−Mo(1)−N(2)	178.90(16)
Mo(1)−P(4)	2.4778(14)	C(13)−N(2)−Mo(1)	130.0(3)
N(1)−O(1)	1.240(5)	C(19)−N(2)−Mo(1)	115.9(3)
N(2)−C(13)	1.373(6)	C(13)−N(2)−C(19)	113.5(4)
N(2)−C(19)	1.468(6)	P(1)−Mo(1)−P(2)	79.88(5)
Mo(2)−N(3)	1.770(4)	P(3)−Mo(1)−P(4)	80.13(5)
Mo(2)−N(4)	2.251(4)	N(3)−Mo(2)−P(5)	84.42(13)
Mo(2)−P(5)	2.4974(13)	N(3)−Mo(2)−P(6)	85.24(14)
Mo(2)−P(6)	2.4592(14)	N(3)−Mo(2)−P(7)	80.89(13)
Mo(2)−P(7)	2.5241(14)	N(3)−Mo(2)−P(8)	90.31(14)
Mo(2)−P(8)	2.4916(14)	N(3)−Mo(2)−N(4)	177.50(17)
N(3)−O(2)	1.230(5)	C(42)−N(4)−Mo(2)	129.9(3)
N(4)−C(42)	1.394(6)	C(48)−N(4)−Mo(2)	115.7(3)
N(4)−C(48)	1.468(6)	C(42)−N(2)−C(48)	113.5(4)
		P(5)−Mo(2)−P(6)	80.07(5)
		P(7)−Mo(2)−P(8)	79.18(5)

dent molecule structures, which allows to conclude that the given arrangement of Figure 7 (Ph approximately in plane with the plane at N2, naphthyl plane approximately perpendicular to it) is a low-energy conformation possessing also a high weight in solution. The two N-bound hydrogens (H19a and H19b) show quite different chemical environments, which are expected to be responsible for the observed splitting of their ^{1}H NMR signals.

Conclusions

Relatively rare insertion reactions of several imines were demonstrated to occur with the activated hydride *trans*-Mo(dmpe)$_2$(H)(NO) producing the corresponding amido complexes. In these reactions *trans*-Mo(dmpe)$_2$(H)(NO) displayed hydride-transfer capabilities presumably due to the strongly polar character of the Mo−H bond.[9] By variation of the type of the inserting imine it became apparent that a supposedly weak Mo−N(amide) bond generates a borderline situation and despite the high reactivity of the hydride applied this may set thermodynamic restrictions to the insertion abilities of the imine component. Superimposed kinetic factors, like the steric congestion in the transition state of the insertion reaction, could also hinder the reaction or even set further limits to the range of applicable inserting imines. Overall the generally high propensity of *trans*-Mo(dmpe)$_2$(H)(NO) to allow hydride-transfer processes provides evidence that ligand tuning may be quite an effective approach to optimize reactivity in transition metal hydride chemistry.[7,15]

Experimental Section

All reactions and manipulations were performed under an atmosphere of dry nitrogen using conventional Schlenk techniques or a glovebox. Solvents were dried according to standard procedures and freshly distilled under nitrogen prior to use. *trans*-Mo(dmpe)$_2$(H)(NO) (**1**) was prepared as described previously.[9] Other reagents were purchased from Fluka or Aldrich. NMR spectra were recorded on the following spectrometers: Varian Gemini-300 instrument, ^{1}H at 300.1 MHz, ^{13}C at 75.4 MHz, ^{31}P at 121.5 MHz, ^{11}B at 96.2 MHz; Bruker DRX-500 instrument, ^{1}H at 500.2 MHz, ^{13}C at 125.8 MHz, ^{31}P at 202.5 MHz, ^{11}B at 160.5 MHz. δ(^{1}H) and δ(^{13}C) are relative to $SiMe_4$, δ(^{31}P) is relative to 85% H_3PO_4, and δ(^{11}B) is relative to BF_3·OEt_2. IR spectra were recorded on a Biorad FTS-45 instrument. Mass spectra were run on a Finnigan-MAT-8400 mass spectrometer. Elemental analyses were performed on a Leco CHN(S)-932 instrument.

***trans*-Mo(dmpe)$_2$(NO)[NPh(CH$_2$Ph)] (2).** A 0.025 g (0.059 mmol) sample of **1** was dissolved in ca. 0.7 mL of C_7D_8. To this solution was added 0.011 g (0.061 mmol) of *N*-benzylideneaniline. After 24 h the reaction was complete (NMR monitoring). The solvent was removed, and the residue was dissolved in ca. 0.5 mL of toluene. Diffusion of pentane into this solution afforded yellow crystals of **2**. Yield: 0.029 g (81%). IR (cm^{-1}, THF): 1538 (NO). ^{1}H NMR (C_6D_6): δ 7.05 (m, 7H, Ph), 6.67 (m, 2H, Ph), 6.47 (t, $^3J_{HH}$ = 7.5 Hz, 1H, Ph), 4.28 (s, 2H, NCH_2), 1.35 (s, 12H, PMe), 1.05 (s, 12H, PMe′), 1.25 (m, 8H, PCH_2). ^{13}C{^{1}H} NMR (C_6D_6): δ 158.9, 144.6, 128.1, 127.4, 127.1, 125.3, 119.5 (br), 110.3 (8 s, Ph), 59.0 (quint, $^3J_{CP}$ = 6.4 Hz, *NCH*$_2$), 30.3 (quint, $^1J_{CP}$ = 10 Hz, *PCH*$_2$), 17.0 (m, PMe). ^{31}P{^{1}H} NMR (C_6D_6): δ 24.8 (s). EI-MS: *m*/*z* 609 (55, M$^+$), 458 (71, [M$^+$ − dmpe]), 426 (88, [M$^+$ − PhCH$_2$NPh]), 396 (22, [M$^+$ − PhCH$_2$NPh − NO]). Anal. Calcd for $C_{25}H_{44}MoN_2OP_4$: C, 49.34; H, 7.30; N, 4.60. Found: C, 49.69; H, 7.33; N, 4.70.

***trans*-Mo(dmpe)$_2$(NO)[NPh(CH$_2$Cp$_2$Fe)] (3).** A mixture of 0.027 g (0.063 mmol) of **1** and 0.022 g (0.076 mmol) of *N*-ferrocenylideneaniline was dissolved in ca. 0.7 mL of C_7D_8 in an NMR tube. The resulting solution was monitored by NMR. After 5 days at room temperature the reaction was complete and the solvent was removed in vacuo. The remaining residue was dissolved in ca. 0.5 mL of benzene. Diffusion of pentane into the benzene solution gave orange crystals of **3**. Yield: 0.037 g (82%). IR (cm^{-1}, THF): 1536 (NO). ^{1}H NMR (C_6D_6): δ 7.24−7.11 (m, 4H, Ph), 6.56 (tt, $^3J_{HH}$ = 6.9 Hz, $^4J_{HH}$ = 1.4 Hz, 1H, Ph), 4.09 (s, 5H, Cp), 4.06 (s, 2H, NCH_2), 3.97 (t, 2H, $^3J_{HH}$ = 2.0 Hz, Cp), 3.84 (t, 2H, $^3J_{HH}$ = 2.0 Hz, Cp′), 1.34 (s, 12H, PMe), 1.08 (s, 12H, PMe′), 1.21 (m, 8H, PCH_2). ^{13}C{^{1}H} NMR (C_6D_6): δ 161.6, 128.5, 127.3, 110.5 (4s, Ph), 120.6 (quint, $^3J_{CP}$ = 3 Hz, Ph), 93.6, 69.2, 68.8, 65.8 (4s, Cp), 53.5 (quint, $^3J_{CP}$ = 6 Hz, NCH_2), 30.3 (quint, $^1J_{CP}$ = 9 Hz, PCH_2), 17.0 (m, PMe). ^{31}P{^{1}H} NMR (C_6D_6): δ 25.1 (s). EI-MS: *m*/*z* 716 (27, M$^+$), 566 (82, [M$^+$ − dmpe]), 426 (34, [M$^+$ − Cp$_2$FeCH$_2$NPh]), 396 (16, [M$^+$ − Cp$_2$FeCH$_2$NPh − NO]). Anal. Calcd for $C_{29}H_{48}FeMoN_2OP_4$: C, 48.61; H, 6.77; N, 3.91. Found: C, 48.93; H, 7.14; N, 3.92.

***trans*-Mo(dmpe)$_2$(NO)[N(Cp$_2$Fe)(CH$_2$Ph)] (4).** A mixture of 0.021 g (0.049 mmol) of **1** and 0.018 g (0.062 mmol) of *N*-benzylideneferrocenylamine was dissolved in ca. 0.7 mL of C_7D_8 in an NMR tube. The resulting solution was heated to 65 °C. After 3 days the reaction was complete (NMR monitoring). The solvent was removed in vacuo. The residue was extracted with diethyl ether.

Table 6. Crystallographic Data and Structure Refinement Parameters for **2**−**5**

	2	**3**	**4**	**5**
formula	$C_{25}H_{44}MoN_2OP_4$	$C_{35}H_{54}FeMoN_2OP_4$	$C_{29}H_{48}FeMoN_2OP_4$	$C_{43}H_{62}MoN_2OP_4$
color	yellow	orange	red	yellow
cryst dimens (mm)	0.36 × 0.27 × 0.21	0.53 × 0.49 × 0.21	0.22 × 0.11 × 0.08	0.27 × 0.20 × 0.11
temp (K)	183(2)	183(2)	123(2)	183(2)
cryst syst	monoclinic	monoclinic	orthorhombic	monoclinic
space group (No.)	P_{21}/n (14)	P_{21}/a (14)	$P_{21}2_12_1$ (19)	P_{21}/c (14)
a (Å)	9.1592(6)	12.2334(8)	9.8225(4)	13.0005(7)
b (Å)	15.9501(7)	14.0645(7)	16.2028(10)	21.3405(14)
c (Å)	20.6001(13)	21.9336(14)	20.5507(9)	31.069(2)
β ($\delta\epsilon\gamma$)	96.615(8)	92.755(8)	90	92.466(8)
V (Å3)	2989.4(3)	3769.5(4)	3270.7(3)	8611.8(10)
Z	4	4	4	8
fw	608.44	794.47	716.36	842.77
d(calcd) (g cm^{-3})	1.352	1.400	1.455	1.300
abs coeff (mm^{-1})	0.673	0.917	1.048	0.487
F(000)	1272	1656	1488	3552
2θ scan range (deg)	5.34 < 2θ < 60.62	5.66 < 2θ < 60.56	5.24 < 2θ < 60.56	3.86 < 2θ < 51.78
no. of unique data	8864	11 191	9700	16 609
no. of data obsd [I > 2s(I)]	6060	8237	7617	8642
abs corr	numerical	numerical	numerical	numerical
solution method	Patterson	Patterson	Patterson	Patterson
no. of params refined	306	365	352	935
R, wR2 (%) all data	4.90, 4.86	5.21, 11.61	4.47, 5.71	9.48, 11.17
R1, wR2 (obsd) (%)[a]	2.75, 4.73	3.53, 9.75	2.98, 5.53	4.70, 10.46
goodness-of-fit	1.030	1.014	1.062	0.993

[a] R1 = $\sum(F_o - F_c)/\sum F_o$, $I > 2\sigma(I)$; wR2 = $\{\sum w(F_o^2 - F_c^2)^2/\sum w(F_o^2)^2\}^{1/2}$.

Concentration and cooling to −30 °C of the extracts afforded **4** as red crystals. Yield: 0.30 g (85.7%). IR (cm^{-1}, THF): 1538 (NO). ^{1}H NMR (C_6D_6): δ 7.31 (d, br, 5H, Ph), 3.88 (s, 4H, Cp), 3.80 (m, 5H, Cp′), 3.34 (s, 2H, NCH_2), 1.40 (m, 8H, PCH_2), 1.30 (s, 12H, PMe), 1.25 (s, 12H, PMe′). ^{13}C{^{1}H} NMR (C_6D_6): δ 144.6, 134.2, 127.9, 126.1 (4s, Ph), 68.3 (s, Cp), 62.3 (quint, $^3J_{CP}$ = 6 Hz Cp′), 60.9 (s, Cp′), 55.8 (quint, $^3J_{CP}$ = 6 Hz, *NCH*$_2$), 30.7 (quint, $^1J_{CP}$ = 10 Hz, *PCH*$_2$), 17.7 (quint, $^1J_{CP}$ = 5 Hz, PMe), 17.2 (quint, $^1J_{CP}$ = 5 Hz, PMe′). ^{31}P{^{1}H} NMR (C_6D_6): δ 24.8 (s). Anal. Calcd for $C_{29}H_{48}FeMoN_2OP_4$: C, 48.61; H, 6.77; N, 3.91. Found: C, 49.01; H, 7.09; N, 3.92.

***trans*-Mo(dmpe)$_2$(NO)[NPh(CH$_2$-1-naphthyl)] (5).** A 0.029 g (0.068 mmol) sample of **1** was dissolved in ca. 0.7 mL of C_7D_8, and 0.017 g (0.073 mmol) of *N*-1-naphthylideneaniline was added. After 6 days at room temperature the reaction was complete (NMR monitoring). The solvent was removed in vacuo, and the residue was recrystallized from diethyl ether at −30 °C to give yellow solid of **5**. Yield: 0.035 g (78%). IR (cm^{-1}, THF): 1540 (NO). ^{1}H NMR (C_6D_6): δ 8.13−6.49 (m, 12H, naphthyl, Ph), 4.84 (s, br, 1H, *NCH*$_2$), 4.57 (s, br, 1H, *NCH*$_2$), 1.34 (s, br, 24 H, PMe), 1.23 (m, 8 H, PCH_2). ^{13}C{^{1}H} NMR (C_6D_6): δ 159.1, 138.4, 134.4, 132.6, 129.6, 126.0, 125.8, 125.4, 125.1, 124.5, 122.8, 110.3 (12 s, naphthyl, Ph), 56.2 (quint, $^3J_{CP}$ = 7 Hz, NCH_2), 30.3 (quint, $^1J_{CP}$ = 9 Hz, PCH_2), 17.0 (br, PMe). ^{31}P{^{1}H} NMR (C_6D_6): δ 24.8 (s). EI-MS: *m*/*z* 659 (40, M$^+$), 508 (50, [M$^+$ − dmpe]), 426 (60, [M$^+$ − $C_{10}H_7CH_2NPh$]), 396 (28, [M$^+$ − $C_{10}H_7CH_2NPh$ − NO]). Anal. Calcd for $C_{29}H_{46}MoN_2OP_4$: C, 52.88; H, 7.05; N, 4.25. Found: C, 53.04; H, 7.06; N, 4.27.

X-ray Crystal Structure Analyses. The intensity diffraction data were collected at 183(2) K (**2**, **3**, **5**) and 123(2) K (**4**) using an imaging plate detector system (Stoe IPDS) with graphite-monochromated Mo Kα radiation. A total of 190, 167, 167, and 220 images were exposed at constant times of 3.00, 1.50, 2.00, and 2.20 min/image for compounds **2**−**5**, respectively. The crystal-to-image distances were set to 50 mm, except of compound **5**, that had a necessary large distance of 70 mm. The corresponding θ_{max} values were 30.31, 30.28, 30.34, and 25.89°, respectively. ϕ-oscillation (**2**, **5**) or rotation scan modes (**3**, **4**) were selected for the ϕ increments of 1.0, 1.2, 1.2, and 0.7° per exposure in each case. Total exposure times for the four compounds were 23, 16, 17, and 23 h in the order of the complexes given above. After integrations and corrections for Lorentz and polarization effects, a total of 7998 reflections for **2**, 7996 for **3** and **5**, and 8000 for **4** were selected out of the whole limiting sphere for the cell parameter refinements. A total of 31 734, 43 436, 34 154, and 49 914 reflections were collected, of which 8864, 11 191, 9700, and 16 609 reflections were unique (R_{int} = 5.22%, 3.85%, 5.23%, and 9.11%); data reduction and numerical absorption correction used 18, 11, 9, and 11 indexed crystal faces.[16]

The structures were solved by Patterson method using the Program SHELXS-97,[17] and they were refined with SHELXL-97.[18] The absolute configuration for **4** was determined by using Flack's *x*-parameter refinement.[19] The absolute structure parameter *x* was 0.538(18); i.e., merohedrical twinning was observed with an appoximate twin ratio of 1:1. The X-ray data collections and the processing parameters are given in Table 6.

Acknowledgment. We are grateful to the Swiss National Science Foundation and the Funds of the University of Zurich for financial support.

Supporting Information Available: Tables of crystal data and structure refinement parameters, atomic coordinates, bond lengths, bond angles, anisotropic displacement parameters, and hydrogen coordinates for **2**−**5**. This material is available free of charge via the Internet at http://pubs.acs.org.

IC030139L

(15) (a) Darensbourg, M. Y.; Ash, C. E. *Adv. Organomet. Chem.* **1987**, *27*, 1. (b) Dedieu, A., Eds. *Transition Metal Hydrides*; VCH Publishers: Weinheim, Germany, New York, 1992. (c) Xin X.; Moss, J. R. *Coord. Chem. Rev.* **1999**, *181*, 27.

(16) *Stoe IPDS software for data collection, cell refinement and data reduction*, versions 2.87−2.92; Stoe & Cie: Darmstadt, Germany, 1997−1999. Verson 2.92 was used for **5**.

(17) SHELXS-97: Sheldrick, G. M. *Acta Crystallogr.* **1990**, *46A*, 467.

(18) SHELXL-97: Sheldrick, G. M. *Programme for the Refinement of Crystal Structures*; University of Göttingen: Göttingen, Germany, 1997.

(19) (a) Flack, H. D. *Acta Crystallogr.* **1983**, *A39*, 876. (b) Flack, H. D.; Bernardinelli, G. *Acta Crystallogr.* **1999**, *A55*, 908.